

Ray and finite-difference modelling of CDP seismic sections for shallow lignite deposits

Johana Brokešová^{a,*}, Jiří Zahradník^b, Paraskevas Paraskevopoulos^c

^a Department of Geophysics, Faculty of Mathematics and Physics, Charles University, Ke Karlovu 3, 121 16 Prague 2, Czech Republic

^b Department of Geophysics, Faculty of Mathematics and Physics, Charles University, V Holešovičkách 2, 180 00 Prague 8, Czech Republic

^c Seismological Laboratory, Section of Applied Geology and Geophysics, Geology Department, University of Patras, Rio 26110, Patras, Greece

Received 4 August 2000; accepted 29 September 2000

Abstract

A numerical experiment carried out to investigate the structural model of the Domenico lignite site is discussed. The model is a 2D structure containing several lignite layers at different depths, and a low-velocity layer at the top of the model. The experiment consists in simulating a measured CDP section by two independent techniques, based on completely different concepts: the finite-difference method and the ray method. Due to the incompleteness of the ray synthetic wave field, as well as to numerical problems of the finite differences at higher frequencies, the agreement between the synthetic seismogram sections for the individual shot points is poor. However, the CDP stacked sections modelled by the ray and finite-difference methods agree rather well. This is because the main differences between the wave fields computed by the two methods are due to the presence of the low-velocity layer (ground roll, head waves, etc.), and just these parts of the wave field can be suppressed by routine data processing such as f - k filtration. Synthetic ray and finite-difference CDP stacks agree relatively well with the observed data. They confirm three lignite seams and a fault in the shallower one. The synthetic data also indicate that many apparent horizons of the measured section may be due to the multiple reflections within the subsurface low-velocity layer. © 2000 Elsevier Science B.V. All rights reserved.

Keywords: Reflection seismics; Lignite; Finite-difference method; Ray method

1. Introduction

Reflection seismic measurements of shallow underground structures are complicated by subsurface low-velocity layers, (e.g., sediments above the

water-table level), and use of the surface sources. As a rule, the weight-drop surface source generates P and S waves with a complicated radiation pattern, and the ground roll is also very strong. Moreover, the high P-velocity contrast at the base of a low-velocity layer gives rise to intensive head waves, whose arrival times may be close to those of the primary reflections from the horizons being investigated. Another complication is due to the extremely high V_p/V_s velocity ratios often encountered close

* Corresponding author.

E-mail addresses: johana@seis.karlov.mff.cuni.cz

(J. Brokešová), jz@karel.troja.mff.cuni.cz (J. Zahradník), paris@geology.upatras.gr (P. Paraskevopoulos).

to the surface, as well as to the highly contrasting velocities and contrasting V_P/V_S velocity ratios at the boundaries between the layers.

All these serious complications contrast with the fact that most exploration work is processed and interpreted under very simplifying assumptions. For instance, the earth is treated as horizontally layered only (1D models) in the acoustic approximation (only P waves being considered, all P–S and S–P conversions being neglected). The reasons for the simplifications are purely practical: exact methods are lacking, or exist but are unstable, and/or time consuming.

In any way, the desirable innovation in this respect is available through seismic modelling based on the combination of various methods. The main purpose of this contribution is to show possible improvements in finite-difference modelling and to offer a new view of the applicability of the ray method to shallow reflection seismics. The finite-difference technique is 'exact' in that it provides the complete wave field containing all realistic wave types. It could be applied in 2D or 3D structures but requires much numerical effort in complex realistic models. The ray method (see, e.g., Červený et al., 1988) is very fast and efficient, flexible and conceptually simple (allowing for identification of the individual body waves) but yields only an approximation of the wave field. The ray synthetic wave field is rather incomplete and may not contain some important waves. These waves may even dominate the seismograms in complex models typical for shallow seismic studies. Only those parts of the wave field that consist of reflections from the most important structural interfaces can be modelled well by the ray method. Therefore, it is useless to compare single-shot synthetic ray and finite-difference wave fields. However, the principal reflections, which can be treated by the ray method, are of great importance in seismic exploration. The routine measurements and subsequent data processing techniques are designed to enhance these parts of the wave field and suppress the others. This gives the ray method a chance to be used with an advantage, e.g., in modelling the CDP stacked sections obtained from the multiple-shot data. Thus, the ray method may contribute significantly to the interpretation of the measured data in complex shallow structures.

The practical goal of this paper (similarly to that in Zahradník and Bucha, 1998) is to provide tools for modelling seismic time sections that would improve the understanding of the recorded wave fields, and help avoid interpretation traps. The object of these studies is the lignite field at the Domenico site in Greece, studied within the NATO SfS project (1995–1998) in close cooperation between the University of Patras and the Charles University.

The proposed structural model, based on the interpretation of real measurements and additional geologic information, is described in Section 2. Sections 3 and 4 concentrate on the numerical aspects of the computational techniques used. In Section 5, synthetic CDP time sections are presented and compared with the sections obtained from the observed data. Conclusions are given in Section 6. Abbreviations FD, ART denote the finite difference and asymptotic ray theory method, respectively. Other often used abbreviations are LVL for low-velocity layer, NLL for non-lignite layer, NMO for the normal moveout, and CDP for the common depth point method of reflection seismology.

2. Description of the model

The structural model used in our numerical study is derived from the measured time section in Fig. 1 and from drilling (Tselentis, personal communication). The structure contains a subsurface LVL, three lignite layers mostly separated from each other by non-lignite layers (NLL), and bedrock. The upper lignite layer is faulted at the left-hand side of the profile. Based on all the available information, a 2D block model suitable for FD modelling was created, see Fig. 2. It was observed at the site that the lignite and non-lignite layers are composed of many thin layers. The problem of the thin-layered structure of the medium in coal exploration studies is addressed, e.g., by Pietsch and Ślusarczyk (1992) or Gochioco (1992). To simplify the model for computations, this detailed structure was not considered and the stacks of the thin layers were replaced by homogeneous layers with average medium parameters.

As we are interested mainly in modelling lignite reflections and not the reflections from the bedrock,

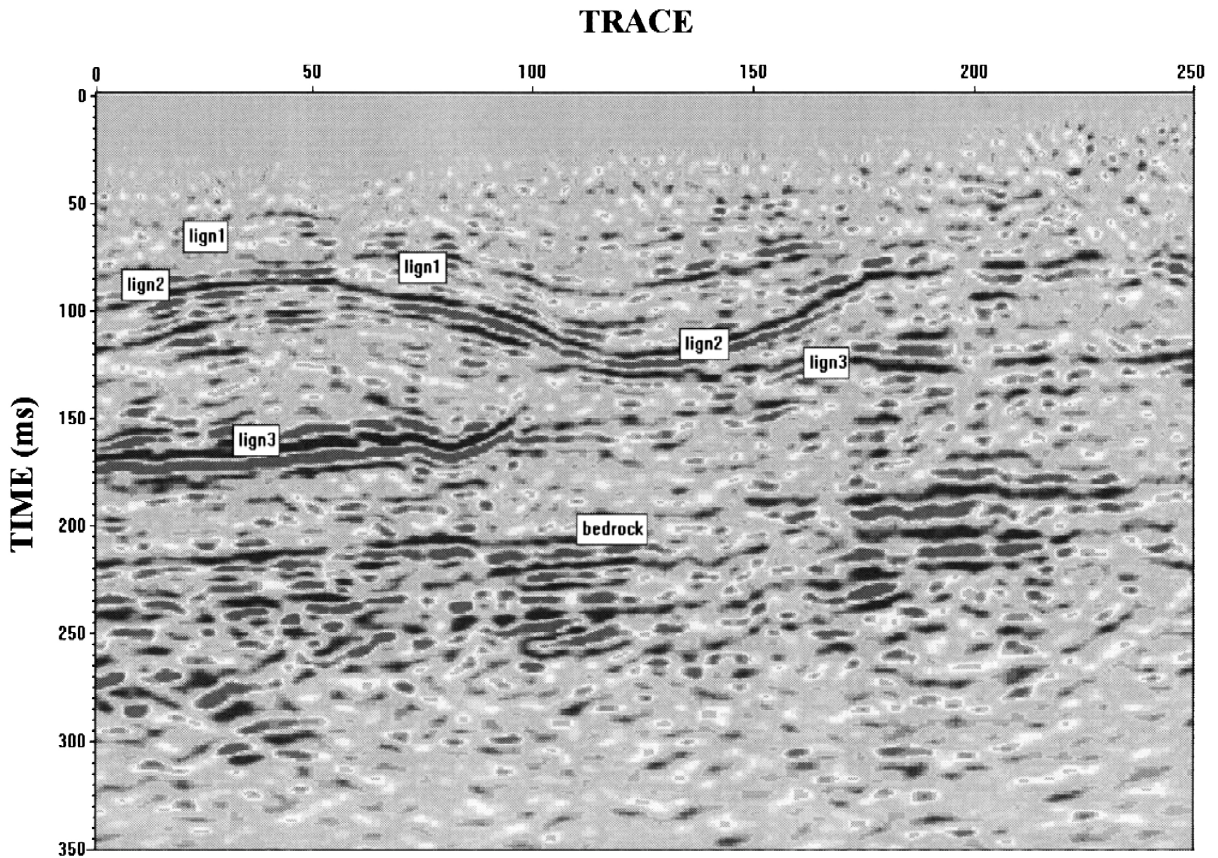


Fig. 1. A selected segment of the true processed CDP time section at the Domenico site (Tselentis, unpublished data). The horizontal range in traces is from 0 (left) to 250 (right) and corresponds to the range 0–625 m. The vertical (time) scale is from 0 to 350 ms. The reflections from the three coal layers and the bedrock are shown.

the bedrock is not included in this model. The numbered layers in Fig. 2 indicate, from above, the LVL with P-wave velocity $V_p = 800$ m/s and the lignite layers ($V_p = 1750$, 1950, and 1850 m/s). As the S-wave velocities are not known well, an approximate V_p/V_s velocity ratio of 4.3 was assumed throughout the entire model. The densities in the individual layers are shown in Table 1.

Since the block model containing sharp interface edges is not suitable for the ray method, a smoothed version of the model, shown in Fig. 3, was used to compute the ray synthetics. The basic shape of the individual layers corresponds well to the measured time section, as well as to the block model used for the FD modeling. In addition to the model in Fig. 2, the structure used for the ART modelling is under-

lain by a medium with $V_p = 3250$ m/s, $V_s = 756$ m/s, $\rho = 2200$ kg/m³ (bedrock). The velocities and densities in the other layers are the same as in the previous model, see Table 1.

The ray and FD models (Figs. 2 and 3) are not identical. In particular, the FD model is composed of polygonal blocks, as formally required by our code. Although blocky models are useful for automated gridding of the medium (Zahradník and Hron, 1992), they complicate this paper, where smooth ray models appear simultaneously. Anyway, this complication is not critical since the main goal of this paper is qualitative comparison between measured time sections and their FD modeling on one side, and between measured time sections and their ray modeling on the other.

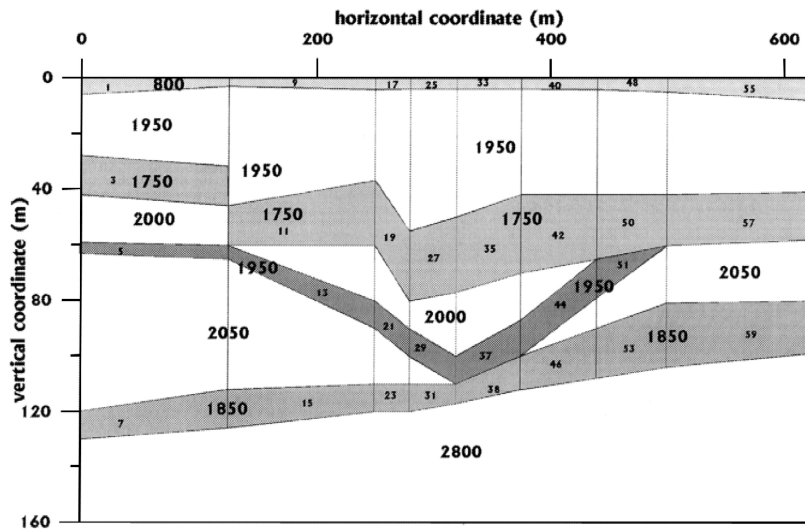


Fig. 2. The structural model constructed from the time section of Fig. 1 and borehole data (Tselentis, pers. comm.), converted to the polygonal model suitable for FD modelling. Small numbers indicate the blocks, large numbers display the P-wave velocities in m/s. Note that the bedrock is not included in this model.

The proposed structural model implies that the seismic modelling for purposes of lignite prospection at the Domenico site is complicated by several factors (most of which are, however, not site-specific):

- non-horizontal lignite layers, including faulted and displaced layers
- several lignite ‘floors’ at different depths
- low-velocity layer (LVL) below surface, with very small velocities, separated by a high-velocity contrast interface from the rest of the model
- very large V_p/V_s velocity ratio

Table 1

Model parameters

Layer	V_p (m/s)	V_s (m/s)	ρ (kg/m ³)
LVL	800	186	1220
1st NLL	1950	453	1520
1st lignite layer	1750	407	1300
2nd NLL	2000	465	1700
2nd lignite layer	1950	453	1450
3rd NLL	2050	477	1750
3rd lignite layer	1850	430	1300
4th NLL	2800	651	1900
Bedrock	3250	756	2200

These factors imply that any seismic modelling that has to include synthetic seismograms for such structures is a difficult task, at the very applicability limit of the existing methods.

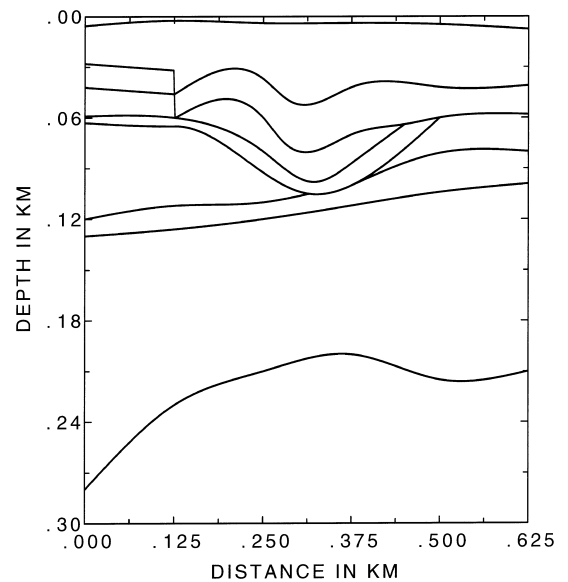


Fig. 3. The structural model used in ART computations (a smooth version of Fig. 2 with minor modifications, complemented by the bedrock at the bottom).

The sources and receivers are located at the free surface of the model. To approximate the weight-drop, used in real measurements, each source is represented by a single force applied vertically. The source-time function is approximated by the Gabor signal. The predominant frequency of the source wavelet is 100 Hz, i.e., the thicknesses of some layers in the model are comparable with the prevailing wavelength.

3. Finite-difference method, PS2 scheme

Shallow deposits are structurally complex, thus requiring robust numerical methods. An important question with regard to the practical applicability of the FD method is: ‘Which features of the elastic finite-difference schemes are essential for their accuracy, and which allow simplifications?’. Zahradník (1995) has shown that the displacement FD schemes employing geometrically averaged parameters are more accurate than those using local material parameters, mainly when a material discontinuity runs between the grid lines. This means that a relatively complex coding of the effective parameters is rewarding.

However, it has been also shown that the accuracy of the mixed spatial derivatives at the internal grid points does not degrade when the number of the implicitly employed stress values and the geometrically averaged material parameters decreases from four to two (the so-called Full and Short Forms, respectively). The Short and Full Forms yield the same numerical results, the Short Form requiring 50% less arithmetic operations. That is the case where simplification is possible at the internal grid-points. However, at the free-surface points such simplification is not allowed, and the Full Form should be used, otherwise a spurious body force is created, and the scheme violates the vanishing-stress condition. Based on these results, a simple elastic scheme (called PS2) has been suggested in Zahradník (1995, Eqs. (3), (10) and (16)).

The PS2 is a second-order scheme in displacements on a regular square grid. Complete 2D elastodynamic equations are solved, thus all P, S and converted waves are considered, including all multi-

ples, head waves, diffracted waves and/or interference waves. The medium is represented as composed of homogeneous polygonal blocks with constant velocities V_p and V_s .

Another advantage of the PS2 scheme is that its flat free-surface treatment (the so-called vacuum formalism) is simple, but, at the same time, it provides an exact proof of approximating zero traction with first-order accuracy.

The reason for focusing much attention on the effective parameters is that sharp coal/rock discontinuities require accurate (non-smoothed, non-shifted) representations, often ignored in literature, although being at least as important as the widely discussed numerical dispersion and/or numerical anisotropy. For warning about the schemes using only point approximations of the elastic parameters (instead of the effective parameters), see Graves (1996), Zahradník et al. (1993) and Moczo et al. (1999).

The V_p/V_s ratio considered in this paper, based on a crosshole measurement at the site, brings modest FD waveform deformations which, however, do not change synthetic time sections qualitatively. For the accuracy analysis of the PS2 scheme at various V_p/V_s ratios, performed by comparison with the finite-element and discrete-wavenumber method, see Opršal and Zahradník (1999) and Moczo et al. (1999), respectively. In general, the V_p/V_s -dependent numerical dispersion complicates in some degree any elastic FD formulation, including for instance all types of the popular staggered formulations (Moczo et al., 2000).

In this numerical study, the FD PS2 scheme was used to simulate the CDP section in two different ways. The first approach, *multiple-shot CDP modelling*, consists in repeated single-shot 2D elastic FD calculations, followed by standard processing (CDP gather, optional f–k filtration, NMO correction and CDP stacking). Note that the analogous multiple-shot CDP approach was also applied to ray synthetics. The second approach, called *array CDP modelling*, requires a single 2D elastic FD calculation of the synthetics excited by a set of sources acting simultaneously at the surface. This approach is relatively inexpensive, but yields only an approximation of the CDP stack.

All FD calculations in this paper were performed with space and time grid steps $dx = 0.5$ m and

$dt = 0.0001$ s, respectively. This grid size yields accurate results for wavelengths above 5 m. For example, for P waves in LVL this is equivalent to frequencies of up to 160 Hz.

4. Computational aspects of the ray method

ART synthetics for the model in Fig. 3 have been computed using the BEAM87 program package (written by V. Červený) designed for 2D complex laterally varying structures. The radiation pattern for a vertical force acting at the earth's surface has been computed using the theoretical formulas of Jílek and Červený (1996), taking into account the presence of the free surface.

The ray synthetic wave field is, in principle, incomplete. The main problems are caused by the LVL in the model. Due to the velocity contrast, the base of the LVL is highly reflective. Consequently, such a layer may act as a waveguide converting a large amount of energy into interference waves travelling along or near the earth's surface (ground roll, head waves). However, these waves, although possibly even dominant in the wave field, cannot be modelled by the zero-order ART. On the other hand, the waves that propagate within the LVL travel at much lower velocity than the waves in the rest of the model, which give us the chance to separate them and filter them out from the wave field.

Another problem connected with the ART synthetics is due to the limited number of elementary waves considered. In the case of a surface source, the ART wave field only consists of far-field P and S body waves reflected from (or, possibly, also converted at) the interfaces. The number of these elementary waves must be limited, otherwise the computational time would increase considerably, mainly due to the necessity of two-point ray tracing for each of these waves. This is another reason why the ART wave field is incomplete. In this way, some of the important multiple reflections, e.g., those connected with the LVL which could be really strong, would be missing in the ray synthetics (do not confuse these multiples with the ground roll in which we are not interested at all). Fortunately, the standard CDP stacking procedure is supposed to suppress the multi-

ples, so that their absence may not be as important in the resulting stacked section.

The ART wave field does not contain diffractions from the edges and unconformities present in the model. Moreover, these structural features can produce shadow zones separated by sharp boundaries from the illuminated parts of the profile. The ART cannot provide any signal, observable in the measured or FD data, penetrating into the shadow zones. The position of the shadow zones, however, changes as the shot point moves along the profile. On the other hand, thanks to a certain robustness of the CDP stacking procedure, such local unrealistic gaps in the ART synthetics may not play an important role in producing the final CDP section. The same holds for the opposite effect to the gaps: locally enhanced amplitudes, e.g., in the vicinity of the caustic points, may also be smoothed by the stack.

5. Synthetic CDP sections

In this section, we present the FD CDP sections, obtained with the two approaches mentioned in Section 3 for the model in Fig. 2 (and its certain modifications). We also present the ART CDP sections for the model in Fig. 3. All these synthetics are plotted in horizontal range from 37.5 to 587.5 m and they are compared with the corresponding measured section.

Fig. 4 shows two multiple-shot FD stacked sections with the shot points spaced at intervals of 62.5 m, the first being situated at $x = 62.5$ m from the left boundary of the model in Fig. 2. The relatively large shot spacing was used in order to keep the computational effort in 'reasonable' limits (one single-shot FD calculation required about 18 h of computational time on a standard Pentium PC). To obtain the stacked FD section, single-shot FD data were optionally f–k filtered, deconvolved, sorted according to CDP numbers, NMO corrected and stacked. The bottom section in Fig. 4 corresponds to the model in Fig. 2, while the section at the top corresponds to the model modified by replacing the LVL by a layer of the same thickness, but filled with the same material as the 1st NLL. In the following such

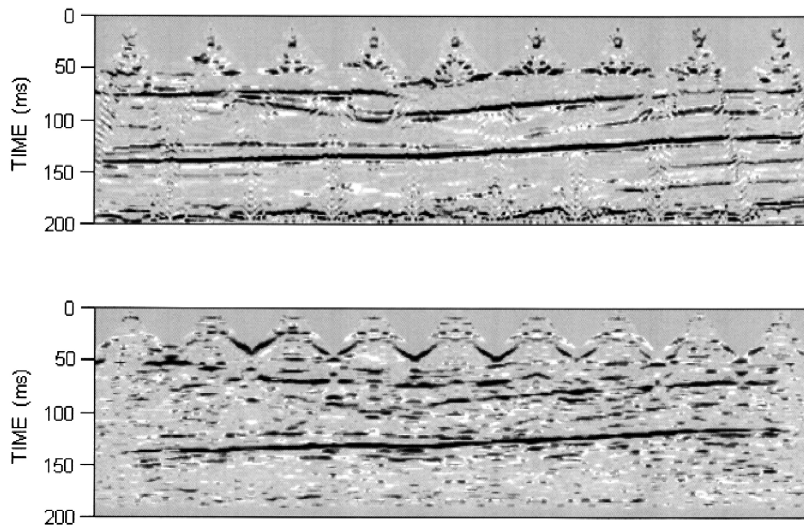


Fig. 4. Multiple-shot FD CDP sections for models without (top) and with (bottom) the LVL. Shot point spacing interval is 62.5 m.

a modified structure is referred to as the *model without LVL*. Comparing both pictures in Fig. 4 we see that the presence of the LVL complicates the wave field reflected from deeper horizons considerably. The data is more noisy and produce more reflections in the final stack. Such undesirable reverberations due to the LVL may obscure the reflections of interest (similar effects have also been reported by Zahradník and Bucha, 1998).

In the following calculations we applied the array FD CDP approach, described in Section 3, to approximate the standard (multiple-shot) CDP section. Fig. 5, in comparison to Fig. 4, demonstrates the accuracy of such an approximation. At the top, there is the section for the model without the LVL, while the bottom panel represents the section for the model with the LVL. We see that the array FD approach models the main reflections very well, with much less numerical effort (only one FD run is required, the computer time of which is similar to that of a single-shot calculation). All the reflections are in their correct positions, and the shallow ones are depicted better (they are stronger) than in the standard CDP stack. Comparing the sections in Figs. 4 and 5, we also see other advantages of the array FD approach: the reflections are more continuous, less noisy and reasonable at the edges (where the stack is not reliable due to insufficient fold coverage). The

effects due to the LVL, mainly the ‘additional’ horizons, are clearly visible in Fig. 5. These reflections are of importance comparable to those from the lignite layers, compared with Fig. 4, bottom, where such additional reflections are much weaker and less continuous.

Thanks to the small computer time requirements of the ray method, it is possible to obtain sufficient CDP fold coverage, and, therefore, it is not necessary to approximate the standard CDP sections by an ‘array ray CDP approach’ similar to that one used in FD computations. The results in Fig. 6 represent the multiple-shot ART modelling of the CDP section for the model in Fig. 3. Twenty shot points spaced at intervals of 25 m, starting from $x = 75$ m, were considered. One single-shot section required only up to 10 min on a standard Pentium PC (compare with the 18 h necessary for the one shot point in the multiple-shot FD approach). The bedrock reflections are not seen within the time window considered in Fig. 6. The time window was chosen to allow for easy comparison with the FD sections in Figs. 4 and 5. The sections for the individual shot points in Fig. 6 were processed similarly as in the case of the multiple-shot FD modelling, i.e., they were f–k filtered, CDP sorted, NMO corrected and CDP stacked. The difference between the top and the bottom part of Fig. 6 is in the number of elementary waves taken

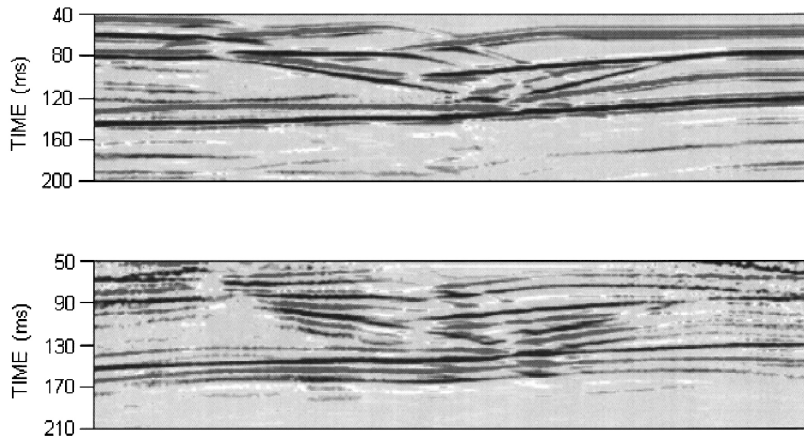


Fig. 5. Array FD CDP sections for the models without (top) and with (bottom) the LVL.

into account. In both sections, the primary P and S reflections from all the interfaces are considered, together with the P–S and S–P waves converted at the reflectors, and some multiple reflections within the lignite layers. Moreover, each deeper reflection is considered together with its ‘ghosts’ generated by the waves reflected (without conversion) *once* from the base of the LVL, either in the vicinity of the source or receiver (the ghost effect). The section in the bottom part of Fig. 6 also includes the multiples reflected *twice* from the bottom of the LVL. The purpose of this numerical experiment was to test

whether the stacking procedure can really suppress the multiples in this particular model. A comparison of the top and the bottom part of Fig. 6 shows that some of the additional multiples remain relatively intensive after stacking. Although they are clearly due to the LVL, they could possibly be misinterpreted as additional lignite layers. Moreover, the experiment suggested that we could not be sure that even other multiples in the LVL (reflected three or more times from the base of the LVL), not included in the ART computations, would be eliminated in the stacked section. Thus, the incompleteness of the

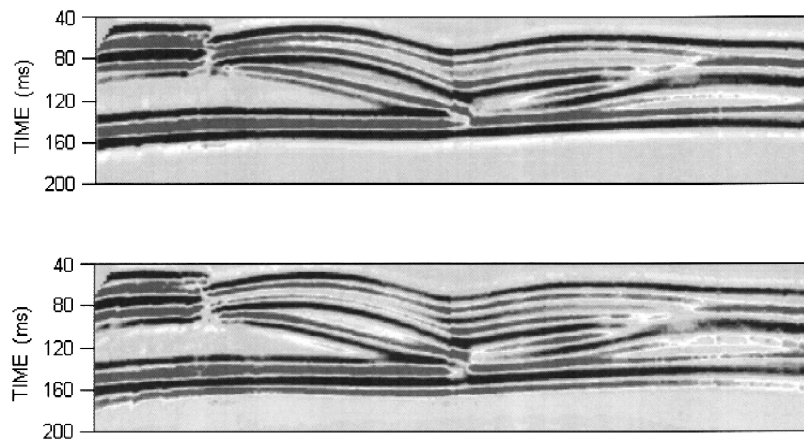


Fig. 6. Multi-shot ART CDP sections for the model in Fig. 3. The bottom part contains some additional multiple reflections within the LVL, see text for details. Shot point spacing interval is 25 m.

ART synthetics may become a serious problem in modelling the proposed structure. But we believe that in models closer to reality as regards absorption (which is not considered in our study), the attenuation would suppress the undesirable reverberations due to the LVL.

In comparing the sections in Figs. 4–6, we have to take into account that the models used in both methods (ART and FD) differ, see Figs. 2 and 3. Since the ART sections in Fig. 6 are stacked (similarly to the multiple-shot FD sections in Fig. 4), the accuracy at the ends of the profile is obviously poor. In those parts with good fold coverage, we can see that, in spite of many limitations of the ART, mentioned in Section 4, the main reflecting horizons, clearly seen mainly in the array FD data, are also present in the ART result.

The next two figures, Figs. 7 and 8, compare synthetics and measured data. Fig. 7 shows the array FD CDP section, including the effects of the LVL (bottom), with the measured data (top). The bottom section of Fig. 7 corresponds better to reality than the top section of Fig. 5 (without the LVL). We clearly see the reverberations due to the LVL. Although they are more continuous, they are similar, at least qualitatively, to those seen in the real stack. The bedrock reflections, seen at the bottom right of the measured data, were deliberately not included in the FD modelling. As expected, the synthetics are clearer (not so noisy) than the measured data. The

reflection marked ‘lign3’ in Fig. 1 is modelled relatively well by the FD approach, at least in the left-hand part of the profile. Reflection ‘lign2’ can also be identified in the FD data, but it is much weaker there. This could be caused by the ‘lign2’ layer being in reality very inhomogeneous, composed of many thin layers (borehole data). These thin layers may enhance the reflection due to some interference effects. Reflection ‘lign1’, although much weaker and obscured by noise in the measured data, also seems to be in the correct position in the FD stack.

Fig. 8 shows the measured data (top) versus the ART CDP section (bottom). In the ART section, only the minimum number of multiple reflections within the LVL was considered (compare Fig. 6). Although the differences between the measured and ART data are significant, we can also see many similarities. For example, the bedrock reflection and the reflection from the 3rd lignite layer on the left-hand side of the profile are modelled relatively well. The ‘lign2’ layer, marked in Fig. 1, can also be found in the ART sections. The ‘lign1’ layer is also seen in the ART synthetics, and even the fault is displayed clearly.

The preliminary interpretation of the measured section offers several possibilities of explaining the strong reflection marked as ‘lign2’ in Fig. 1. One possibility is the existence of a lignite layer (2nd lignite layer in Table 1), but other interpretations are

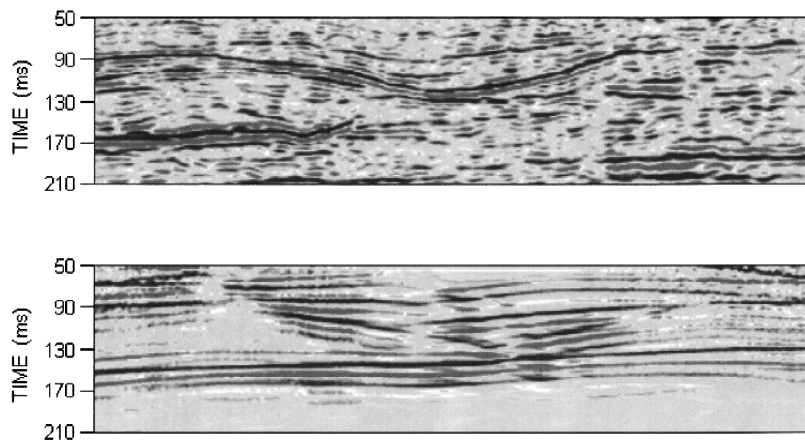


Fig. 7. The real stacked section (top) and the array FD CDP section for the model in Fig. 2, including the LVL (bottom).

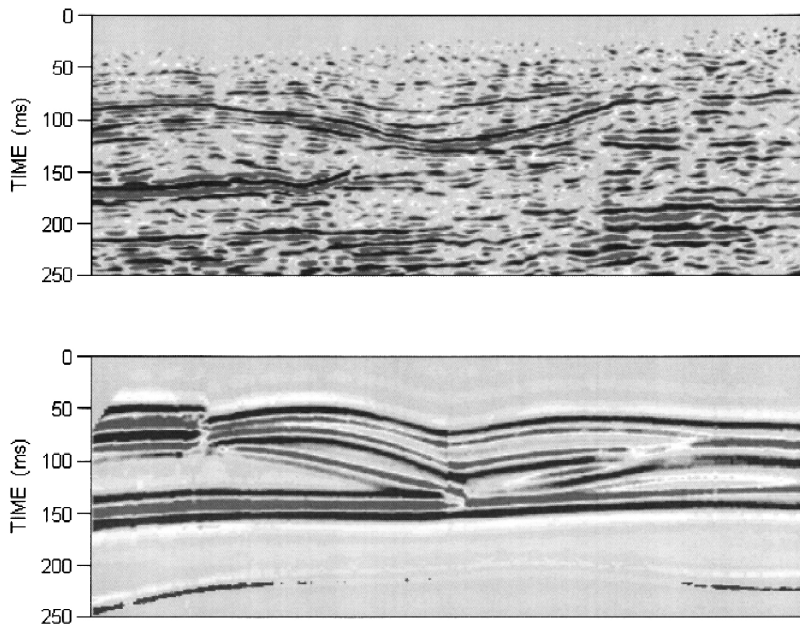


Fig. 8. The real stacked section (top) and the multiple-shot ART CDP stack, with smaller number of multiples within the LVL (bottom).

also possible (e.g., the effect of converted waves reflected from the 'lign1' layer, etc.). One of the

objectives of our computations was to contribute to this problem. In Fig. 9, top, we have considered the

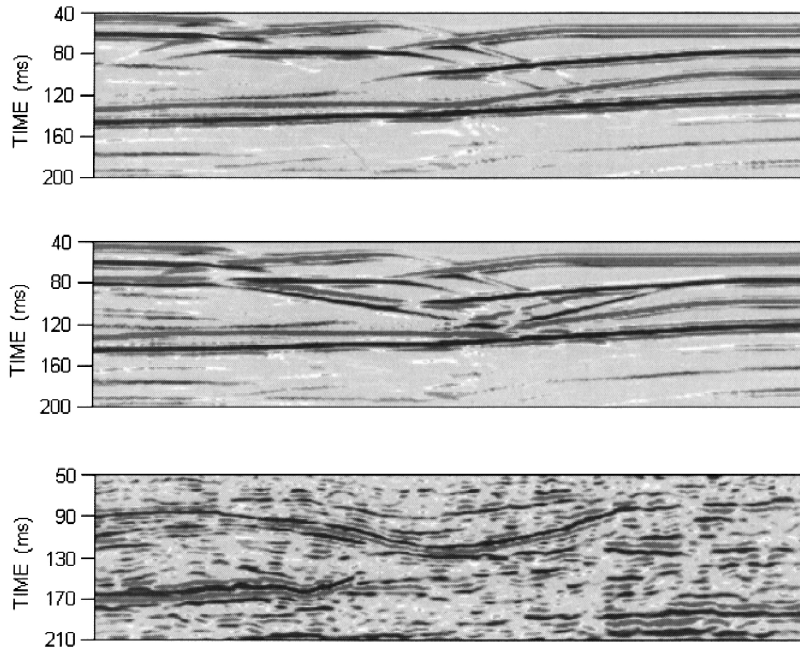


Fig. 9. The array FD CDP sections for the models without LVL and without (top) and with (middle) the 2nd lignite layer compared with the real CDP stack (bottom).

FD block model but without the 2nd lignite layer, i.e., the layer was replaced by the same material as that in the 2nd NLL in Table 1. Fig. 9, middle, corresponds to the FD block model of Fig. 2 (i.e., including the 2nd lignite layer). The figure allows us to identify the reflections from the top and base of the 2nd lignite layer. On comparing the synthetics in Fig. 9 top and middle with the measured section (Fig. 9, bottom), we can conclude that the section including the 2nd lignite layer is closer to the real CDP stack. This suggests that ‘lign2’ does exist in reality. This conclusion can be supported by also taking into account ray synthetics (Figs. 6 and 8) where 2nd lignite layer could be identified too.

6. Concluding remarks

The presented numerical study resulted both in certain site-specific findings and in several methodical conclusions applicable to elastic modelling of shallow lignite deposits. Let us summarize them briefly as follows.

(1) The multiple-shot FD CDP sections resemble the measured section in many respects.

(2) The array FD modelling is an efficient approximation of the multiple-shot FD stack. Its cost is the same as that of a single-shot FD calculation.

(3) The array FD modelling yields a clearer section than the multiple-shot FD stack. This perhaps makes the section too simple compared to the “noisy” multiple-shot FD stack, thus resembling more the ART result. However, this allows the individual horizons in the FD stack to be identified more easily.

(4) Since the ray modelling is very fast, multiple-shot CDP stacks for a very large number of shot points can be produced much more easily in the ART than in FD modelling. Neither is a long time window a principal problem for the ART. The multiple-shot coverage smoothens the singularities of the ART wave field. Some of the LVL effects, such as multiple reflections from the base of the LVL, can also be modelled by the ART, but at the price of dramatically increasing computer time.

(5) Considering the complexity of the studied model, it may be surprising that the ART CDP stacks display many similarities with the FD stacks (in particular with the array FD stacks).

(6) At the Domenico site, both the ART and FD sections indicated the existence of the intermediate “lign2” layer, as well as the presence of a fault in the 1st lignite layer.

(7) The synthetic models also indicate that many apparent horizons of the measured section may be due to the LVL effects that cannot be eliminated by routine processing because of lateral heterogeneities. The LVL may also obscure the picture of the shallowest lignite layer.

Acknowledgements

The authors thank G.A. Tselentis, director of Seismological Laboratory, University of Patras, for supporting this work and providing the data within the NATO Science for Stability Programme, the GR-COAL grant. This work has been partially supported also by the Czech Republic Grant Agency (205/00/0902), and the NATO Science Fellowship of the first author. The authors wish to thank to K. Žáček for technical assistance with final adjustment of figures.

References

- Červený, V., Klimeš, L., Pšenčík, I., 1988. Complete seismic ray tracing in three-dimensional structures. In: Doornbos, D.J. (Ed.), *Seismological Algorithms*. Academic Press, New York, pp. 89–168.
- Gochioco, L.M., 1992. Modeling studies of interference reflections in thin-layered media bounded by coal seams. *Geophysics* 57, 1209–1216.
- Graves, R.W., 1996. Simulating seismic wave propagation in 3D elastic media using staggered-grid finite differences. *Bull. Seismol. Soc. Am.* 86, 1091–1106.
- Jílek, P., Červený, V., 1996. Radiation patterns of point sources situated close to structural interfaces and to the Earth’s surface. *PAGEOPH* 148, 175–225.
- Moczo, P., Lucká, M., Kristek, J., Kristeková, M., 1999. 3D displacement finite differences and a combined memory optimization. *Bull. Seismol. Soc. Am.* 89, 69–79.
- Moczo, P., Kristek, J., Halada, L., 2000. 3D 4th order staggered-grid finite-difference schemes: stability and grid dispersion. *Bull. Seismol. Soc. Am.* 90, in press.
- Opršal, I., Zahradník, J., 1999. From unstable to stable seismic modeling by finite-difference method. *Phys. Chem. Earth (A)* 24, 247–252.

- Pietsch, K., Ślusarczyk, R., 1992. The application of high-resolution seismics in Polish coal mining. *Geophysics* 57, 171–180.
- Zahradník, J., 1995. Simple elastic finite-difference scheme. *Bull. Seismol. Soc. Am.* 85, 1879–1887.
- Zahradník, J., Hron, F., 1992. Robust finite-difference scheme for elastic waves on coarse grids. *Studia Geoph. Geod.* 36, 1–19.
- Zahradník, J., Bucha, V., 1998. Masking effects of subsurface layers on shallow reflecting horizons. *J. Seismol. Explor.* 7, 73–79.
- Zahradník, J., Moczo, P., Hron, F., 1993. Testing four elastic finite-difference schemes for behaviour at discontinuities. *Bull. Seismol. Soc. Am.* 83, 107–129.